Catalysis Today 452 (2025) 115242

Contents lists available at ScienceDirect

Catalysis Today

journal homepage: www.elsevier.com/locate/cattod

H_2 production from photocatalytic reforming of PET over Pt/TiO_2: The role of terephthalic acid

Luke Roebuck [a,*], Min Hu [a], Helen Daly [a], Hubertus Warsahartana [a], Louise S. Natrajan [b], Arthur Garforth [a], Carmine D'Agostino [a,c], Marta Falkowska [a], Christopher Hardacre [a,*]

[a] Department of Chemical Engineering, School of Engineering, The University of Manchester, M13 9PL, United Kingdom
[b] Department of Chemistry, School of Natural Sciences, University of Manchester, Manchester M13 9PL, United Kingdom
[c] Dipartimento di Ingegneria Civile, Chimica, Ambientale e dei Materiali (DICAM), Alma Mater Studiorum – Università di Bologna, Via Terracini, 28, Bologna 40131, Italy

ARTICLE INFO

Keywords:
PET
Plastics valorisation
Depolymerization
Photoreforming
Hydrogen production
TiO_2
Waste-to-energy

ABSTRACT

Photoreforming is a promising method for the conversion of waste materials with simultaneous production of H_2. The use of waste polyethylene terephthalate (PET) as a photoreforming substrate has been previously investigated, however its insolubility in aqueous media and the resistance of the aromatic terephthalate towards conversion are major obstacles. Commonly an alkaline pretreatment step is used to initiate hydrolysis to ethylene glycol and terephthalic acid which promotes H_2 evolution. However, in this work we have found that TPA has both promotional and inhibitory effects by modification of the catalyst surface that depend on the relative concentration of ethylene glycol. Terephthalic acid inhibits the oxidation reactions by scavenging hydroxyl radicals and blocking complexation sites. This leads to lower H_2 evolution compared to the photoreforming of an equivalent concentration of ethylene glycol. Even in trace amounts, terephthalic acid would still inhibit the reaction unless the concentration of ethylene glycol was high enough. Surprisingly, at ethylene glycol concentrations of > 1.2 M, residual terephthalic acid promoted the reaction which is thought to be due to increasing the interaction between ethylene glycol and the catalyst surface but also an increased role of water. On the basis of these results, we suggest that, if PET is to be used as a feedstock for H_2 generation by photoreforming, an initial hydrolysis should be performed after which terephthalic acid is separated for re-use. The remaining hydrolysate may then be used for photoreforming. Furthermore, the ethylene glycol concentration should be maximized in order to overcome the inhibitory effects of residual terephthalic acid.

1. Introduction

Plastic waste is one of the foremost environmental concerns of our time. The issue largely originates from poor management of waste streams and the resistance of man-made polymers towards natural degradation. Chemical recycling of plastic waste is a promising route to addressing the plastic waste issue. This approach involves the chemical depolymerisation of plastics back to their monomers followed by repolymerisation. This is highly desirable as plastics with "as new" properties can be produced compared with traditional recycling approaches [1]. Depolymerised waste plastics may also be employed to produce other value-added products or fuels [2,3]. Polyethylene terephthalate (PET) is the highest production volume polymer worldwide mostly used in plastic bottles, food packaging, and textiles. Global production of PET exceeded 36 million tons in 2023 and is expected to continue to increase [4]. Therefore, chemical recycling or depolymerisation strategies are indispensable to reduce the environmental impact in terms of plastics waste produced but also reducing the demand on increasingly limited crude oil resources. Chemical recycling towards converting PET back to monomers ethylene glycol and terephthalic acid via hydrolysis type depolymerisation has been demonstrated. However, large excesses of water are often needed that may cause difficulty in separation of soluble products such as ethylene glycol. Conversion to other valuable monomers such as dimethyl terephthalate (DMT) [5] or *para*-xylene have also been shown to be possible [6].

As an energy vector, H_2 will play a critical role in the net-zero transition [7,8]. However, new sustainable production methods and new sustainable feedstocks utilised to produce H_2 that can compete

* Corresponding authors.
E-mail addresses: luke.roebuck@manchester.ac.uk (L. Roebuck), c.hardacre@manchester.ac.uk (C. Hardacre).

https://doi.org/10.1016/j.cattod.2025.115242
Received 30 September 2024; Received in revised form 14 January 2025; Accepted 13 February 2025
Available online 14 February 2025

economically with steam methane reforming are desperately needed. Photocatalytic reforming (photoreforming) has been researched extensively to degrade pollutant or waste materials while producing H_2 [9,10]. Typically, this is performed under mild reaction conditions *i.e.* ambient temperature and pressure in aqueous solvent. Photoreforming makes use of semiconductor photocatalysts which oxidise organic materials *via* hydroxyl radicals releasing protons which are then reduced to form H_2. From an economic standpoint, waste polymers would be an ideal feedstock for hydrogen generation through photoreforming [11]. Uekert *et al.* have studied the photoreforming of PET using CdS/CdO_x and $CN_x|Ni_2P$ photocatalysts to produce H_2 as well as value added products [12,13]. Other carbon nitride based photocatalysts have also been the subject of investigation for this application [14–17]. However, a number of issues with this depolymerisation recycling strategy exist. Firstly with the polymer being a solid, the incident light, which has to reach the surface of a photocatalyst for the reaction to proceed, can be strongly scattered reducing the penetration depth and this drastically limits the concentration of polymer that can be used. Secondly, when solid substrates are used, the reaction kinetics are severely limited due to poor contact between substrate and catalyst. As a result, an alkaline pretreatment step is often employed to hydrolyse PET to its monomers (ethylene glycol and terephthalic acid (TPA)) (Scheme 1). Furthermore, TPA is largely resistant to photodegradation due to its aromatic ring and contributes very little to the overall H_2 produced [12]. As a known scavenger of hydroxyl radicals, TPA may also inhibit the photoreforming reaction [18]. In this work we investigate these issues and propose methodologies to combat them. In particular, we propose that TPA is separated prior to photoreforming. As TPA has a low solubility (0.065 g L^{-1} at 25 °C) it is easily separated by filtration from the post-reaction mixture. Separation of TPA may be a more economically viable approach as it can then be then re-used for polymerization back to PET or utilised for other purposes [19,20]. The remaining hydrolysate is then subjected to photoreforming to eliminate the remaining monomer and recover energy in the form of H_2. By employing this strategy, it is possible to recover TPA, a valuable product which may be then re-used, and optimise the production of H_2.

2. Experimental

2.1. Chemicals and materials

PET powder was prepared by grinding of virgin PET granules (RAMAPET N1S, Indorama Ventures) in a coffee grinder and sieved to achieve a final particle size of 250–425μm. 15 wt% $Pt(NO_3)_4$ precursor solution, hydrochloric acid (37 %), and nitric acid (70 %), were obtained from Alfa Aesar/Thermo Fischer. Terephthalic acid (>99 %) was purchased from Acros Organics. Ethylene glycol (99.8 %), glycolaldehyde, paraformaldehyde (95 %), and platinum standard solution (1000 mg ml^{-1}) were purchased from Sigma-Aldrich®. Formic acid (99 %) was purchased from Fluorochem. Commercially available TiO_2 support Aeroxide® P25 was obtained from Evonik. Paraformaldehyde was used to prepare formaldehyde solutions by dissolution in deionised water at 60 °C. All other chemicals were used as received with no further treatment. Deionised water (18.2 MΩ) was used for all experiments which was obtained from the Direct-Q 3UV ultrapure water system (Millipore®).

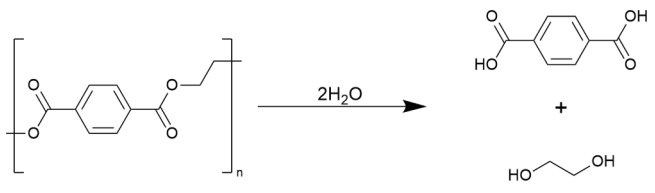

Scheme 1. Hydrolysis of polyethylene terephthalate to its monomers: ethylene glycol and terephthalic acid.

2.2. Catalyst synthesis

The 0.2 wt% Pt/TiO_2 (P25) photocatalyst for photoreforming reactions was prepared by the wet-impregnation method. 2 g of P25 TiO_2 was suspended in 20 ml of deionised water with magnetic stirring with heating at 60 °C. The appropriate amount of $Pt(NO_3)_4$ precursor solution to achieve the target final metal loading was then added dropwise to the suspension of the TiO_2 support. The mixture was then allowed to evaporate to dryness over 4 h with continuous stirring. The impregnated catalyst was then dried at 150 °C for 1 h and then calcined in static air at 500 °C for 2 h with a heating rate of 5 °C min^{-1}. Finally, the catalyst was reduced in a flow of pure H_2 (99.99 %, BOC) at 200 °C for 1 h with a heating rate of 5°C min^{-1} using a tube furnace.

2.3. Catalyst Characterisation

The specific surface area of the prepared catalyst was analysed by N_2 adsorption/desorption at 77 K using a Micromeritics ASAP 2020 instrument and the Brunauer-Emmett-Teller (BET) model. X-ray diffraction (XRD) patterns were obtained using a Bruker D2 Phaser diffractometer with a CuK_α ($\lambda = 0.154$ nm) radiation source. Measurements were collected over a range of 2θ from 10° to 90° with a step size of 0.02°. The actual metal loading of the catalyst was measured by inductively coupled plasma with optical emission spectroscopy (ICP-OES) using a Analytik Jena PlasmaQuant PQ 9000 Elite instrument. Emission lines were monitored at 270.2, 283.0, and 299.8 nm corresponding to Pt. The instrument was calibrated using five Pt standard solutions covering the expected loading range. Prior to measurement the catalyst was dissolved in a mixture of concentrated HCl and HNO_3 (3:1 ratio) by microwave digestion at 200 °C for 20 min using an ETHOS EASY system and then diluted to 25 ml.

2.4. Photocatalytic reactions

For PET photoreforming reactions in Section 3.2, 300 mg of PET powder was suspended in 30 ml of 2 M KOH and stirred for 24 h at 60 °C. This mixture was then either used as a photoreforming substrate as is, or the undissolved PET was filtered out. In one experiment TPA was precipitated out using HCl and filtered out of the mixture along with the undissolved PET. For reactions in Section 3.3, an appropriate volume of ethylene glycol was diluted to 30 ml with deionised water. To these mixtures 2.5 mg of TPA was added in certain experiments, as detailed in Section 3.3. Following preparation of these mixtures, they were transferred to an 80 ml flat-bottomed borosilicate glass reactor along with 30 mg of Pt/TiO_2 photocatalyst. The reactor was then sealed and purged with argon for 30 min in order to remove any dissolved gasses. The reactor was then irradiated with a UV LED array (12 V, SMD3528, $\lambda =$ 365–375 nm). A gas line from the headspace of the reactor was fitted to allow for venting of the gas during purging and to allow continuous online gaseous sampling at regular time intervals. The gaseous phase products were analysed using an Agilent 8860 online gas chromatograph (GC) system equipped with thermal conductivity detector (TCD) and flame ionisation detector (FID) using Porapak Q and HayeSep D columns in series. Liquid phase samples were taken manually at regular intervals using a syringe through a septum in the reactor. The liquid samples were then analysed using an Agilent 1220 Infinity II HPLC system with refractive index (RI) and UV-diode array detection (DAD) ($\lambda =$ 210 nm) using an Agilent HC-C18(2) column with methanol as the mobile phase. For HPLC analysis 2 M HCl was added to a 0.5 ml aliquot of reaction mixture to precipitate TPA. The resultant mixture was then diluted in a 5 ml volumetric flask with methanol to redissolve the TPA. For samples without significant TPA (Section 3.3) samples were measured without any sample preparation using a BioRad Aminex HPX-87H column with a 5 mM H_2SO_4 mobile phase. Calibration curves for

each of the analysed compounds were prepared by measuring standard solutions of the pure compounds at 5 different concentrations covering the expected range.

2.5. Fluorescence spectroscopy

Samples of the reaction mixtures (20 ml) were taken at the end of the reaction and filtered to separate the catalyst. The catalyst was then washed with dilute NaOH to remove any terephthalic acid bound to its surface. The filtrate was then made up to a 25 ml standard dilution in volumetric flasks. Steady state emission and excitation spectra were recorded on an Edinburgh Instruments FLS-1000 photoluminescence spectrometer equipped with a 450 W steady state xenon lamp with double 325 mm focal length excitation and emission monochromators in Czerny Turner configuration. All spectra were corrected in the excitation and emission mode using the detector correction files (in built to the Edinburgh Instruments software) to account for variations in the excitation lamp profile and detector sensitivity across the visible spectrum. All scan parameters were identical for all samples and all samples were measured on the same day to minimise errors.

2.6. ζ-Potential measurements

ζ -potential was measured using a Malvern Zetasizer Nano instrument utilizing electrophoretic light scattering. The Pt/TiO_2 catalyst was dispersed in aqueous ethylene glycol solutions of different concentrations in the range 0.3 M to 1.2 M with and without addition of TPA. The catalyst amount was fixed at 1 mg ml^{-1} to match the amount used in the photoreforming reactions. The dispersions were injected into disposable folded capillary cells. Samples were equilibrated for 20 s prior to measurement. Measurements were taken at 25 °C.

2.7. NMR relaxation

^1H NMR relaxation measurements were performed using a Magritek SpinSolve benchtop NMR spectrometer with a ^1H frequency of 43 MHz. All measurements were performed under ambient pressure and temperature. The spin-lattice (T_1) and spin-spin (T_2) relaxation times were measured using a T_1-T_2 pulse sequence [21]. The samples were prepared by soaking the catalyst particles in a series of EG solutions with or without TPA, for 48 h. Then the samples were removed from the liquids and put on a filter paper and gently dried to remove excess liquids on the external surface. After that, the samples were transferred to 5 mm NMR tubes for measurement.

3. Results and discussion

3.1. Characterisation results

The prepared Pt/TiO_2(P25) catalyst had a specific surface area of 40.4 m^2 g^{-1} calculated using the BET model from low temperature (77 K) N_2 adsorption data. The catalyst was also found to have a BJH pore volume of 0.11 cm^3 g^{-1}. Adsorption/desorption isotherms can be found in Figure S2. Analysis of XRD patterns (Figure S2) of the impregnated catalyst revealed that the TiO_2(P25) support contained 19.6 % rutile phase with the remainder anatase phase. Phase composition was determined on the basis of the relative intensities of the rutile (110) and anatase (101) reflections using a method that has been described elsewhere [22]. Using ICP-OES after microwave digestion of the catalyst in aqua regia, it was determined that the actual platinum loading was 0.23 wt%, slightly higher than the target loading of 0.20 wt %.

3.2. Photoreforming of PET

Photocatalytic reforming reactions were performed using PET and PET pretreated in 2 M KOH. The H_2 evolution rates and conversions for these reactions are shown in Fig. 1. Without any pretreatment, photoreforming of PET resulted in only 8.1 % conversion after 8 h irradiation and low H_2 and CO_2 evolution rates of 0.12 and 0.09 mmol g^{-1} h^{-1} respectively. This is only marginally higher than the rate of pure water splitting (Figure S3). No liquid phase products could be detected in the reaction mixture after irradiation as they are degraded at a much higher rate than they are produced. Pretreatment for 24 h in 2 M KOH led to a significant increase in conversion, as expected. After 24 hrs pretreatment in 2 M KOH, 10.9 % of PET was converted, after photoreforming, a total of 32.2 % was converted after 8 h irradiation. Therefore, during photoreforming 21.3 % PET was converted, which is significantly higher than without pretreatment in KOH. This increased conversion during photoreforming may be due to the reduced particle size after pretreatment or associated with the alkaline conditions making. the surface of the polymer more susceptible to attack by oxidising species. During the irradiation the H_2 evolution rate was increased from 0.12 to 0.6 mmol g^{-1} h^{-1}. No CO_2 was evolved due to the alkaline conditions where it is sequestered as the carbonate. Prior to irradiation, the pretreated PET mixture contained 10 mM ethylene glycol and 16 mM terephthalic acid and no other hydrolysis products such as 2-hydroxyethyl terephthalic acid (MHET) or bis(2-hydroxyethyl) terephthalate (BHET) could be detected. After 8 h of irradiation the ethylene glycol concentration had decreased by 25 % forming glycolaldehyde. The amount of terephthalate decreased from 16 mM to 11 mM. No C1 oxidation products such as formic acid or formaldehyde were detected. In comparison, the photoreforming of the equivalent concentration of 10 mM pure ethylene glycol resulted in a H_2 evolution rate of 3.2 mmol g^{-1} h^{-1} (Figure S3). This reduction in photoreforming rate may be due to the light scattering of undissolved PET or inhibitory effects of TPA.

To investigate the cause of the lower H_2 evolution compared to the equivalent concentration of ethylene glycol two further reactions were performed. After pretreatment of the PET, photoreforming of the solution following filtration of undissolved PET was compared with the solution following removal of both PET and TPA by filtration. In the latter case, the TPA was precipitated with HCl and filtered out together with the PET. Thus, these reaction mixtures contained ethylene glycol and TPA (10 mM and 16 mM respectively) and ethylene glycol (10 mM) only together with other minor hydrolysis products. It can be seen from Fig. 1

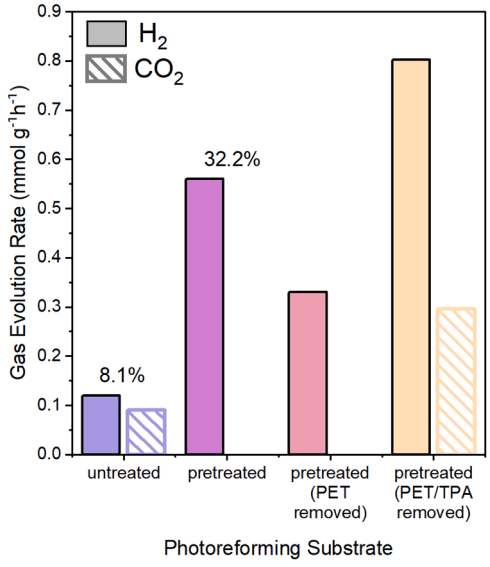

Fig. 1. Evolution rates of H_2 and CO_2 from the photoreforming of PET, pretreated PET, and PET hydrolysate (all 10 mg ml^{-1} PET) with TPA removed. % Conversion of PET is shown above the untreated and pretreated samples gas evolution bars. Reaction conditions: 30 ml reaction volume, 30 mg Pt/TiO_2 photocatalyst, UV (λ = 365–375 nm) irradiation, 8 h reaction time.

that the H_2 evolution from the sample with PET removed had decreased to 0.33 mmol g^{-1} h^{-1} compared with the unfiltered solution indicating that H_2 must also be evolved directly from PET during photoreforming under alkaline conditions as well as from the hydrolysis products. Furthermore, this shows that the light scattering effect of unreacted PET is insignificant at this concentration. However, when both PET and TPA are removed, the H_2 evolution increased to 0.80 mmol g^{-1} h^{-1} Due to the neutralisation of KOH by HCl, CO_2 was also evolved at a rate of 0.30 mmol g^{-1} h^{-1}. The neutralisation of alkaline conditions may in part explain this increase in H_2 production as KOH is inhibitory but KCl is not (Figure S3). However, this does not fully account for the increase observed. Unlike in previous reactions, formic acid and formaldehyde were produced with 0.2 and 2 mM of each present in the final reaction mixture. This shows that when the TPA is removed, the conversion of glycolaldehyde is able to proceed. This more efficient oxidation is likely to correspond to a higher rate of H_2 production. The reason for the low reaction rates for the KOH-pretreated PET was not the availability of reactants or light scattering but primarily due to inhibitory effects of the TPA. This is also demonstrated in Fig. 2. In the PET hydrolysate where TPA had been separated by filtration, small quantities of dissolved TPA remain as it has a solubility of 0.065 g L^{-1}. The effect of this residual TPA can be observed as the H_2 evolution from photoreforming of the hydrolysate is still significantly lower than that of an equivalent concentration of pure aqueous ethylene glycol (Figure. S3). Furthermore, as TPA itself is relatively unreactive under photoreforming conditions (Figure. S3), separation of the TPA compared with photoreforming is more sustainable and economic. The lack of C1 products in the final reaction mixture indicate that C-C cleavage reactions were not taking place in the pretreated PET sample. We hypothesise that this was due to the evolved terephthalate blocking complexation sites on the TiO_2 surface required for this type of reaction [23,24]. This is supported by the observation that after photoreforming of the PET hydrolysate with TPA removed, significant quantities of C1 oxidation products of ethylene glycol were produced. It must be noted however, that the comparing concentrations of liquid phase intermediates between reactions that are under acidic or basic conditions are not fully indicative of mechanism as different degrees of hydration, dissociation, and binding to the catalyst can occur.

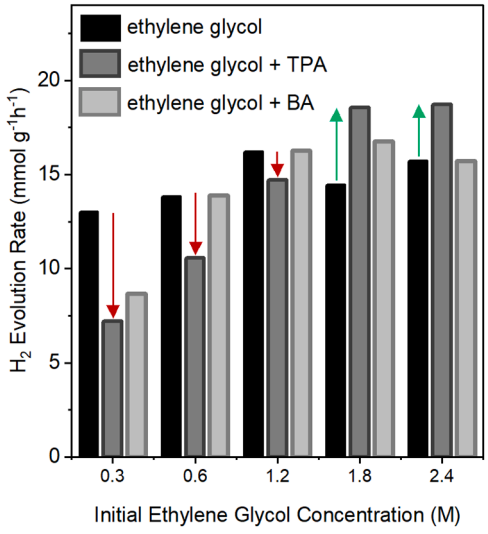

Fig. 2. H_2 evolution rate vs. initial ethylene glycol concentration with and without the presence of TPA and BA after 4 h UV irradiation over Pt/TiO_2. Reaction conditions: 30 ml reaction volume, 30 mg Pt/TiO_2 photocatalyst, UV (λ = 365–375 nm) irradiation, 4 h reaction time. Arrows represent the change in rate from the reaction without TPA to the reaction with TPA.

3.3. *Effect of terephthalic acid on ethylene glycol photoreforming*

The results in the previous section suggested that even trace amounts of TPA left in the reaction mixture following separation by filtration could inhibit the photoreforming reactions. To test this, photoreforming reactions were performed using ethylene glycol with an amount of TPA added that was in slight excess of its solubility limit in water (2.5 mg) to mimic the residual amount that would remain in solution after filtration. Furthermore, it was also hypothesised that increasing the ethylene glycol concentration could be used to overcome the inhibitory effect of the residual TPA. Therefore, photoreforming reactions were also performed with higher ethylene glycol concentrations. The hydrogen evolution rates for these reactions vs the equivalent reactions without TPA are shown in Fig. 2. As anticipated, the extent of the inhibition decreases as the ethylene glycol concentration is increased. Remarkably however, when the ethylene glycol concentration was increased to 1.8 M the H_2 evolution rate was promoted by 29 % when TPA was present from 14.4 to 18.5 mmol g^{-1} h^{-1}. At 2.4 M the reaction was also promoted however to a slightly lesser extent with a 19 % increase from 15.7 to 18.7 mmol g^{-1} h^{-1}. The small increase in rate between 1.8 M and 2.4 M suggests that the ethylene glycol is approaching saturation of the catalyst surface. Previous studies have shown that the first oxidation step on Pt/TiO_2 (P25) involves the abstraction of an α-hydrogen from physisorbed ethylene glycol by a hydroxyl radical to form glycolaldehyde as shown in Scheme 2 [23]. Subsequent reaction steps require chemisorption/complexation to occur. Therefore, it is probable that the first reaction step could be inhibited by TPA scavanging hydroxyl radicals but subsequent reaction steps may be also inhibited by strongly bound TPA blocking adsorption sites. In order to gain deeper insight into the inhibition/promotion mechanism the concentrations of liquid phase products at the end of the reaction were analysed (Fig. 3). It can be seen that the concentrations of all intermediates are lower when TPA is present except for glycolaldehyde when the initial ethylene glycol concentration is above 1.8 M. In this case the glycolaldehyde increased by 24 % at 1.8 M and 19 % at 2.4 M which can be correlated with the increase in H_2 evolution rate. Therefore, it can be concluded that the increase in the rate of the first oxidation step is a source of the promoted H_2 evolution. The role of water may also be a factor; however this is difficult to determine from the stoichiometry of the intermediates and will be address in subsequent sections. When no TPA is present this first reaction step (Fig. 3(a)) follows a Langmuir-Hinshelwood type relationship *i.e.* where the reaction is 1st order at low concentrations; however, as the concentration is increased the reaction approaches zero order and the curve begins to plateau. This corresponds to the surface of the catalyst becoming saturated with reactant molecules [25]. However, when TPA is present the plateau in the rate-concentration relationship appears to be shifted towards higher concentrations. This suggests that the TPA increases the amount of ethylene glycol that the catalyst is able to adsorb which consequently increases the reaction rate. This behaviour was not observed for formaldehyde or formic acid where their concentrations are not increased, meaning that the promotional effect relates to the initial conversion of ethylene glycol to glycolaldehyde only. On the basis of these findings, for H_2 production to be maximised when using PET as a photoreforming substrate, hydrolysis methods that are capable of higher degrees of conversion are needed. This would produce higher concentrations of ethylene glycol which could overcome the inhibitory effects of TPA and potentially even, under the correct concentration ratios, promote the reaction. Steam hydrolysis is one such method that can readily convert PET in high yields under mild reaction conditions [19,20]. Steam hydrolysis was used to produce a hydrolysate that could be used as a photoreforming substrate. A high conversion of 99 % was achieved; however, when this was photoreformed the H_2 evolution rate was low (Figure S4). It was found that despite the high degree of PET conversion, there was significant soluble oligomeric species present that may have inhibited the reaction (Figure S5). Therefore, the hydrolysis reaction must also be optimised to reduce the

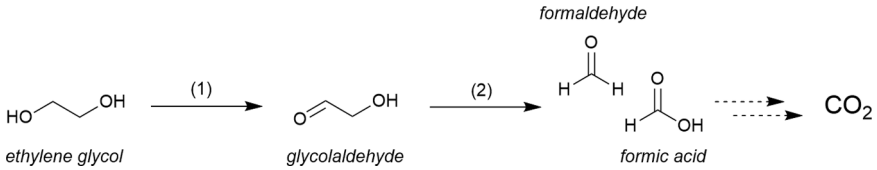

Scheme 2. Photooxidation pathway of ethylene over Pt/P25 under anaerobic conditions. Step (1) H-abstraction from ethylene glycol by hydroxyl radicals (indirect mechanism). Step (2) C-C cleavage by direct hole transfer to chemisorbed glycolaldehyde.

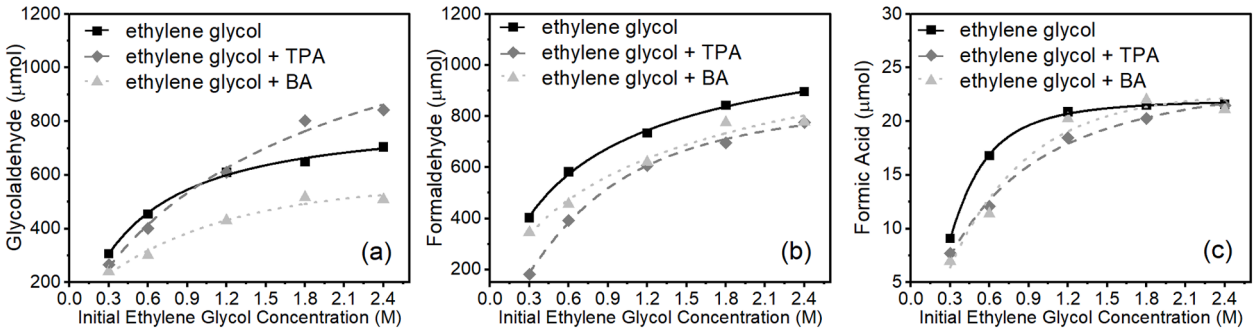

Fig. 3. Concentrations of liquid phase intermediates (a) glycolaldehyde, (b) formaldehyde, and (c) formic acid vs initial ethylene glycol concentration with and without the presence of TPA and BA. Reaction conditions: 30 ml reaction volume, 30 mg Pt/TiO_2 photocatalyst, UV (λ = 365–375 nm) irradiation, 4 h reaction time.

quantities of these oligomers in order to improve H_2 evolution. This is, however, outside the scope of the present work and will be the subject of future investigations.

In order to probe the nature of the TPA interaction with the catalyst surface, the results were compared with those using benzoic acid (BA) (Fig. 2) as it has a similar structure but a single carboxylic group (*vs.* two in TPA). The presence of the same concentration of BA (3.2 mg) had a lesser effect than TPA. At low ethylene glycol concentration (0.3 M) the reaction was inhibited but not as much as with TPA. At the intermediate concentrations (0.6 M and 1.2 M) the was no difference in H_2 evolution compared to the photoreforming of ethylene glycol without BA. At 1.8 M ethylene glycol there was a small promotion in H_2 evolution which then disappeared at 2.4 M. In the presence of BA the concentrations of all reaction intermediates were decreased (Fig. 3). BA is known to scavenge hydroxyl radicals in a similar manner as TPA however to a lesser extent [26]. This being the reason why less inhibition occurs compared to when TPA is present. This supports the hypothesis that TPA scavenges radicals leading to a lower quantity of oxidising species being available for degradation of ethylene glycol. While site blocking could also occur inhibiting later reaction steps. The finding that BA also promotes the reaction at 1.8 M ethylene glycol, but less significantly, suggests that the second carboxylic acid group of TPA is influencing the reaction in some way. Carboxylic acids will bind strongly to the TiO_2 surface through the formation of carboxylates. For BA only one monodentate carboxylate formation is possible; however, in the case of TPA multiple adsorption modes are possible. The adsorption mode of TPA on TiO_2 has previously been demonstrated to depend on surface coverage [27]. At low surface coverages TPA adsorbs with both acid groups bound to the TiO_2 surface whereas at higher coverages it is adsorbed through only one acid group. As the TPA coverage is in the high coverage range, therefore, the TPA is likely to adsorb in an upright manner with the second acid unbound and, therefore, free to influence the reaction *via* hydrogen bonding or aiding proton transfer [28].

3.4. Radical scavenging effect of TPA

In order to test the hypothesis that TPA is scavenging hydroxyl radicals and thus affecting oxidation of ethylene glycol, fluorescence spectroscopy was employed. Upon reaction with a hydroxyl radical TPA forms 2-hydroxyterephthalic acid (TPA-OH) which is fluorescent [29]. This method has widely been used as an analytical technique in the quantitative determination of hydroxyl radial formation [18,30,31]. Therefore, fluorescence spectroscopy can be used to determine the extent of radical scavenging by TPA which is not itself fluorescent. The fluorescence spectra from the final reaction mixtures from Section 3.3 are shown in Fig. 4. The emission peak centred at approximately 420 nm using an excitation wavelength of 325 nm is characteristic of TPA-OH. This clearly shows that in all reactions studied, hydroxyl radicals are being scavenged by TPA and therefore less are available for oxidation of ethylene glycol. Interestingly, as ethylene glycol concentration is increased, the concentration of TPA-OH decreases and therefore, the extent of radical scavenging by TPA decreases. This indicates that as the surface coverage of ethylene glycol increases it begins to out-compete TPA for the hydroxyl radicals. As ethylene glycol can be completely mineralized to CO_2 resulting in the release of all of its protons, this results in a higher H_2 production rate when it is oxidized vs TPA. When TPA is consuming the radicals, only one proton is released per molecule as it is not oxidized further than TPA-OH [29]. This finding clearly shows that the competition for hydroxyl radicals between TPA and ethylene glycol is the primary cause of the changes in H_2 evolution seen in Fig. 2. However, it does not fully explain the why the reaction is promoted by TPA above 1.2 M ethylene glycol. Even if ethylene glycol was able to fully outcompete TPA for radicals it would be expected that the H_2 production would simply return to the level seen without the presence of TPA. Clearly another mechanism is present. As previously discussed, it appears that the TPA increases the adsorption of ethylene glycol on the basis of the rate-concentration relationship of the first reaction step.

3.5. Surface interaction of ethylene glycol in the presence of TPA

Clearly the presence of TPA bound to the surface of the Pt/TiO_2 catalyst has significant impact on the photoreforming reaction. In particular the interaction of reactants with the catalyst and oxidation mechanisms are altered. The changes strongly depend on the concentrations of both TPA and reactants. Despite inhibiting the reaction at lower concentrations, surface bound TPA is proposed to increase the adsorption of ethylene glycol on the catalyst surface. This increased adsorption results in a promotion of the H_2 evolution rate at higher concentrations of ethylene glycol (>1.2 M). It seems that the increased

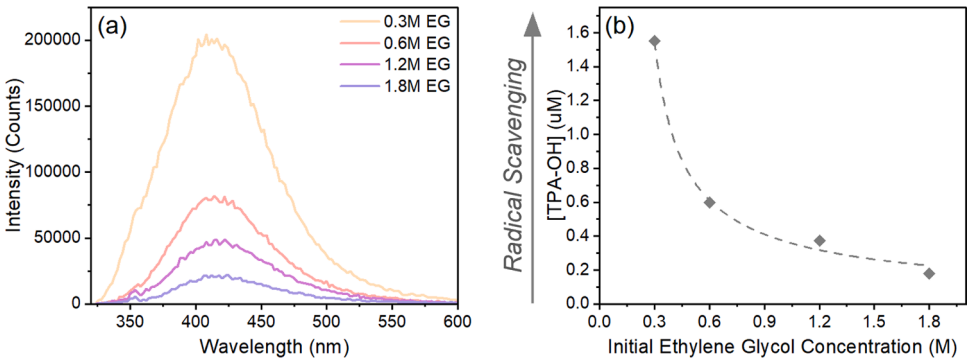

Fig. 4. Corrected steady state fluorescence spectra of post reaction mixtures from the photoreforming of ethylene glycol at different initial concentrations diluted in water over Pt/TiO_2 in the presence of TPA. Excitation wavelength = 325 nm corresponding to the absorption and excitation of TPA-OH and characteristic emission centred at 420 nm.

adsorption can overcome the inhibiting effects of TPA seen at lower concentrations. In other words, when the surface concentration of ethylene glycol is high enough it can outcompete TPA for hydroxyl radicals. As the surface concentration of ethylene glycol is likely to be higher when TPA is present than on the bare catalyst at the same bulk concentration then the reaction is promoted. In this section we study these surface interactions in more detail.

Surface charging is one of the most important factors in determining adsorption [32] therefore we have investigated the effect of TPA on the surface charging of the Pt/TiO_2 catalyst. Fig. 5 shows the ζ-potential of the catalyst with and without adsorbed TPA in ethylene glycol solutions (0.3 M-1.8 M) at native pH. It can be seen that ζ-potential increased significantly to more positive values when TPA is present indicating modification of the catalyst surface [33]. The shift of ζ-potential in the positive direction can be explained by the transfer of protons from the second acid group to the surface hydroxyls which are then protonated [34]. This supports the previous assumption that TPA is bound to the surface *via* a single acid group. Furthermore, a positive surface charge should promote the adsorption of ethylene glycol by electrostatic interaction with the partial negative charge of the oxygen atoms. This may in part explain the promotional effect of TPA.

The interaction of the substrates with the catalyst surface can also be probed using the NMR T_1/T_2 ratio, that is, the ratio of the longitudinal-to-transverse nuclear spin relaxation times, which is indicative of strength of surface interactions [21]. This method has previously been applied in a number of studies to determine the relative strength of interaction between an adsorbate molecule and a catalyst surface [35–37]. For example, D'Agostino et al. have employed this method investigate the relationship between the oxidation of diols over oxide supported metal catalysts and their adsorption strength [38,39]. Therefore NMR relaxation measurements were used here to study the

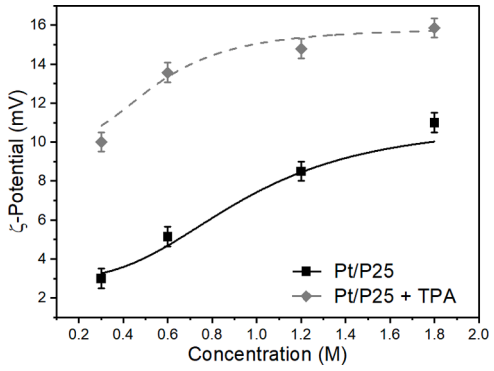

Fig. 5. ζ -potential of Pt/TiO_2 catalysts in reaction mixture before irradiation with and without TPA at different ethylene glycol concentrations.

interaction of ethylene glycol and the Pt/TiO_2 catalyst and assess how addition of TPA modifies this interaction. Solutions of 0.8, 1.2 and 1.8 M were used for NMR measurements, below 0.8 M no ethylene glycol peak could be observed due to the much larger excess of water solvent dominating the NMR signal in the T_1-T_2 maps. The T_1/T_2 relaxation ratios for different ethylene glycol concentrations are shown in Fig. 6. The smaller of the two peaks (A) represents the aliphatic hydrogen of ethylene glycol whereas the larger peak (B) represents signal from water protons and protons of the hydroxyl group of ethylene glycol. Given the large excess of water, this peak is mostly dominated by water. A minor tail of this peak can be noted, which is likely to arise from the presence of ethylene glycol hydroxyl groups.

A first observation is that for the system in the absence of TPA an increase in ethylene glycol concentration leads to generally higher T_1/T_2 ratio for such species, a trend that is generally similar to that observed for the catalytic activity shown in Fig. 2, hence suggesting that the adsorption of ethylene glycol over the surface plays an important part in determining the overall catalytic activity in this case. As for the behaviour of the system without and with TPA, it is possible to note a major difference between the two systems when considering the T_1/T_2 ratio of water as a function of ethylene glycol concentration. This is displayed in Fig. 7, which shows that for the system with TPA an increase in ethylene glycol concentration leads to a sharp increase of the T_1/T_2 ratio of water relative to that of ethylene glycol, whereas in the absence of TPA an opposite trend is observed, that is, the relative T_1/T_2 ratio decreases with increasing ethylene glycol concentration. In addition, it is possible to note that for ethylene glycol concentrations of 0.8 and 1.2 M, the T_1/T_2 ratio of water relative to that of ethylene glycol in the absence of TPA is higher than the case with TPA; however, at 1.8 M there is a switch between the two systems and such a ratio becomes higher for the case with TPA. This trend seems to reflect well the trend observed for catalytic data in Fig. 2 and suggests that water plays an important part in the reaction, in particular the results suggest that when TPA is added to the system a higher affinity of the catalyst surface with water is beneficial. We hypothesise that the higher affinity for water on the TiO_2 surface in the presence of TPA results in a higher degree of hydroxyl radical production via oxidation of the adsorbed water [40]. A higher degree of hydroxyl radical production would promote the oxidation of ethylene glycol to glycolaldehyde which is a radical driven process [23]. This is clearly seen in Fig. 3(a) where in the presence of TPA glycolaldehyde is formed in higher quantities when an initial ethylene glycol concentration of 1.8 M and above is used. This reaction step is key in determining overall H_2 production rate.

The increased interaction for both ethylene glycol and water may in part be caused by electrostatic effects where dissociative adsorption of TPA leads to protonation of surface hydroxyls and a more positively charged catalyst particle indicated by the increased ζ -potential. However as the promotional effect with BA occurs to a lesser extent than

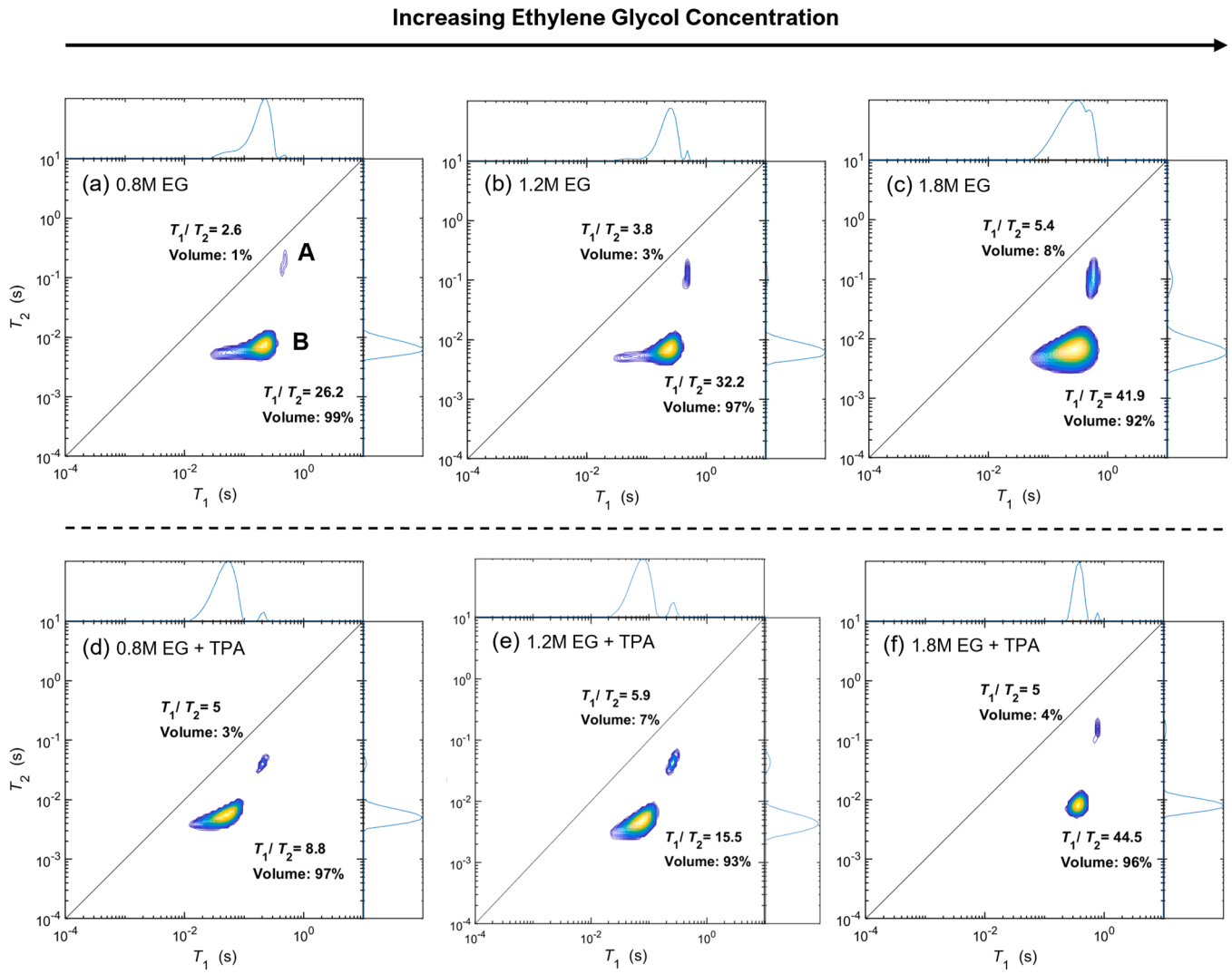

Fig. 6. ^{1}H NMR T_1-T_2 correlation data for ethylene glycol over Pt/TiO_2 without TPA (a-c) and with TPA present (d-f) at ethylene glycol concentrations of 0.8, 1.2, and 1.8 M.

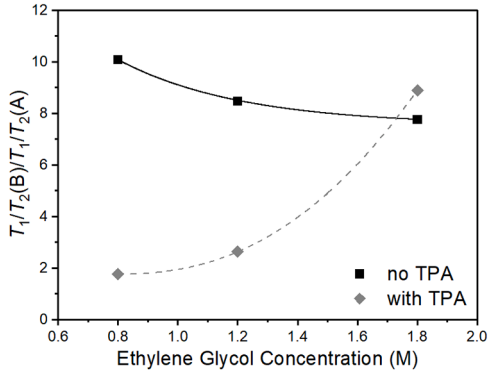

Fig. 7. Ratio of T_1/T_2 values of water peak (B) vs aliphatic ethylene glycol peak (A) from ^{1}H NMR.

TPA, it seems that the second acid group also has an impact on the interaction between ethylene glycol and the catalyst. Hydrogen bonding between the acid group of TPA and ethylene glycol may play a crucial role. It has been shown elsewhere that modification of catalyst surfaces with carboxyl or boronic acid groups increase the conversion of cellulose by hydrogen bonding to the hydroxyl groups of cellulose [41,42]. Furthermore, the formation of hydrogen bonding networks of reactant molecules at the catalyst surface has been shown to increase the photooxidation of water and methanol [43–45].

4. Conclusions

In this study it was found that utilising an alkaline pretreatment step significantly enhanced the H_2 evolution from the photoreforming of PET. However, TPA in the hydrolysate was found to inhibit the reaction. When alkali pretreated PET is used directly the TPA inhibits the breakdown of ethylene glycol into smaller C1 intermediates and CO_2 limiting the amount of H_2 evolved. The H_2 production was enhanced further by separating out the TPA formed prior to photoreforming. However, even when residual amounts of TPA were present in the reaction mixture after filtration, the H_2 evolution was still lower than the photoreforming of an equivalent concentration of pure aqueous ethylene glycol. The primary cause of this inhibition effect was due to the radical scavenging nature of TPA as revealed through fluorescence spectroscopy. The initial oxidation of ethylene glycol is a hydroxyl radical driven process and therefore is inhibited by the presence of TPA. Subsequent reaction steps that require chemisorption of the reactants were also inhibited by TPA blocking adsorption sites. Interestingly however, when the ethylene glycol concentration was increased to 1.8 M and above, the H_2 evolution was promoted by the presence of

TPA. NMR relaxometry revealed that this was due to increased interaction of ethylene glycol with the catalyst when its surface chemistry was modified by TPA. Furthermore, when ethylene glycol concentration was increased, the relative affinity of water towards the surface increased dramatically. We hypothesize that this results in a greater production of hydroxyl radicals through water oxidation which then promotes ethylene glycol oxidation and ultimately H_2 production. At ethylene glycol concentrations of 1.8 M and above it appears that this modified surface behaviour could overcome the inhibitory effects of the TPA. This work has shown that there is a balance to be considered when utilising PET as a feedstock for H_2 generation by photoreforming. If pretreated PET is used directly, H_2 can be generated without the simultaneous evolution of CO_2. However, conversion is sluggish, and a mixture of organic products remain in the liquid phase, these products may or may not be useful and are likely difficult to separate. We propose that if PET were to be used commercially as a feedstock for H_2 generation then it should be depolymerized first and the TPA component separated and re-used. As TPA is largely unreactive towards photoreforming, and is wasted if not separated, we believe this is a more viable strategy. In particular, this strategy may be useful, in depolymerized PET streams that are too dilute for viable recover of ethylene glycol or to repolymerise. The TPA may then be used for other purposes such as conversion to other value-added chemical such as para-xylene or used in the synthesis of MOFs. The depolymerization may be an alkaline pretreatment step as shown in this work or by other means such as thermal hydrolysis processes which are able to fully convert the PET [19, 20]. Following this approach H_2 generation can be maximised, a useful product in TPA can be recovered, and PET can be degraded more efficiently, all under very mild reaction conditions.

CRediT authorship contribution statement

Falkowska Marta: Writing – review & editing, Supervision. **D'Agostino Carmine:** Writing – review & editing, Resources, Methodology, Formal analysis. **Garforth Arthur:** Supervision, Resources. **Natrajan Louise S.:** Resources, Methodology, Funding acquisition. **Warsahartana Hubertus:** Investigation. **Daly Helen:** Supervision, Investigation, Conceptualization. **Hu Min:** Visualization, Investigation, Formal analysis. **Roebuck Luke:** Writing – original draft, Visualization, Investigation, Formal analysis, Conceptualization. **Hardacre Christopher:** Writing – review & editing, Supervision, Funding acquisition, Conceptualization.

Declaration of Competing Interest

The authors declare that they have no known competing financial interests or personal relationships that could have appeared to influence the work reported in this paper.

Acknowledgements

The authors thank the Supergen Bioenergy Hub funded by EPSRC Grant (EP/S000771/1) for support provided. We also gratefully acknowledge the resources provided from our membership of the UK Catalysis Hub Consortium funded by EPSRC Grants: EP/R026939/1, EP/R026815/1, EP/R026645/1 and EP/R027129/1. We acknowledge access to the EPSRC funded NNUF CRR National Nuclear Users Facility EP/T011289/1 for access to the Edinburgh Instruments FLS-1000 spectrometer. M. Hu and C. D'Agostino acknowledge EPSRC Grant EP/V026089/1. S. Zainal is thanked for assistance in generation of NMR graphs. A. Nadri is acknowledged for support with experimental work and instrument training. Sarayute Chansai is also acknowledged for assistance in the set-up of the online-GC system.

Appendix A. Supporting information

Supplementary data associated with this article can be found in the online version at doi:10.1016/j.cattod.2025.115242.

Data availability

Open access data is available at https://doi.org/10.48420/28417877.

References

[1] A. Rahimi, J.M. García, Chemical recycling of waste plastics for new materials production, Nat. Rev. Chem. 1 (2017) 0046, https://doi.org/10.1038/s41570-017-0046.
[2] P.S. Roy, G. Garnier, F. Allais, K. Saito, Strategic approach towards plastic waste valorization: challenges and promising chemical upcycling possibilities, ChemSusChem 14 (2021) 4007–4027, https://doi.org/10.1002/cssc.202100904.
[3] F. Zhang, F. Wang, X. Wei, Y. Yang, S. Xu, D. Deng, Y.-Z. Wang, From trash to treasure: chemical recycling and upcycling of commodity plastic waste to fuels, high-valued chemicals and advanced materials, J. Energy Chem. 69 (2022) 369–388, https://doi.org/10.1016/j.jechem.2021.12.052.
[4] GlobalData, Polyethylene Terephthalate (PET) Industry Capacity and Capital Expenditure Forecasts with Details of All Active and Planned Plants to 2028, ⟨https://www.globaldata.com/store/report/polyethylene-terephthalate-market-analysis/⟩, 2024 (accessed May 2024).
[5] Z.T. Laldinpuii, V. Khiangte, S. Lalhmangaihzuala, C. Lalmuanpuia, Z. Pachuau, C. Lalhriatpuia, K. Vanlaldinpuia, Methanolysis of PET waste using heterogeneous catalyst of bio-waste origin, J. Polym. Environ. 30 (2022) 1600–1614, https://doi.org/10.1007/s10924-021-02305-0.
[6] J. Li, Z. An, Y. Kong, L. Zhang, J. Yang, X. Wang, J. Wang, D. Duan, Q. Zhang, R. Long, D.G. Vlachos, Z. Li, Selective recovery of para-xylene from polyethylene terephthalate plastic, Appl. Catal. B-Environ. Energy 357 (2024) 124307, https://doi.org/10.1016/j.apcatb.2024.124307.
[7] S. French, The role of zero and low carbon hydrogen in enabling the energy transition and the path to net zero greenhouse gas emissions, Johns. Matthey Technol. Rev. 64 (2020) 357–370, https://doi.org/10.1595/205651320X15910225395383.
[8] H. Kouchaki-Penchah, O. Bahn, H. Bashiri, S. Bedard, E. Bernier, T. Elliot, A. Hammache, K. Vaillancourt, A. Levasseur, The role of hydrogen in a net-zero emission economy under alternative policy scenarios, Int. J. Hydrog. Energy 49 (2024) 173–187, https://doi.org/10.1016/j.ijhydene.2023.07.196.
[9] A. Patsoura, D.I. Kondarides, X.E. Verykios, Photocatalytic degradation of organic pollutants with simultaneous production of hydrogen, Catal. Today 124 (2007) 94–102, https://doi.org/10.1016/j.cattod.2007.03.028.
[10] B. Rico-Oller, A. Boudjemaa, H. Bahruji, M. Kebir, S. Prashar, K. Bachari, M. Fajardo, S. Gómez-Ruiz, Photodegradation of organic pollutants in water and green hydrogen production via methanol photoreforming of doped titanium oxide nanoparticles, Sci. Total Environ. 563-564 (2016) 921–932, https://doi.org/10.1016/j.scitotenv.2015.10.101.
[11] M. Ashraf, N. Ullah, I. Khan, W. Tremel, S. Ahmad, M.N. Tahir, Photoreforming of waste polymers for sustainable hydrogen fuel and chemicals feedstock: waste to energy, Chem. Rev. 123 (2023) 4443–4509, https://doi.org/10.1021/acs.chemrev.2c00602.
[12] T. Uekert, M.F. Kuehnel, D.W. Wakerley, E. Reisner, Plastic waste as a feedstock for solar-driven H_2 generation, Energy Environ. Sci. 11 (2018) 2853–2857, https://doi.org/10.1039/C8EE01408F.
[13] T. Uekert, H. Kasap, E. Reisner, Photoreforming of nonrecyclable plastic waste over a carbon nitride/nickel phosphide catalyst, J. Am. Chem. Soc. 141 (2019) 15201–15210, https://doi.org/10.1021/jacs.9b06872.
[14] X. Gong, F. Tong, F. Ma, Y. Zhang, P. Zhou, Z. Wang, Y. Liu, P. Wang, H. Cheng, Y. Dai, Z. Zheng, B. Huang, Photoreforming of plastic waste poly (ethylene terephthalate) via in-situ derived CN-CNTs-NiMo hybrids, Appl. Catal. B 307 (2022) 121143, https://doi.org/10.1016/j.apcatb.2022.121143.
[15] S. Guo, Y. Huang, D. Li, Z. Xie, Y. Jia, X. Wu, D. Xu, W. Shi, Visible-light-driven photoreforming of poly(ethylene terephthalate) plastics via carbon nitride porous microtubes, Chem. Commun. 59 (2023) 7791–7794, https://doi.org/10.1039/D3CC02012F.
[16] M. Li, S. Zhang, Tandem chemical depolymerization and photoreforming of waste PET plastic to high-value-added chemicals, ACS Catal. 14 (2024) 2949–2958, https://doi.org/10.1021/acscatal.3c05535.
[17] W. Wang, S. Song, P. Wang, M. He, Z. Fang, X. Yuan, H. Li, C. Li, X. Wang, Y. Wei, W. Song, H. Xu, Z. Li, Chemical bonding of g-C3N4/UiO-66(Zr/Ce) from Zr and Ce single atoms for efficient photocatalytic reduction of CO2 under visible light, ACS Catal. 13 (2023) 4597–4610, https://doi.org/10.1021/acscatal.2c06255.
[18] G. Žerjav, A. Albreht, I. Vovk, A. Pintar, Revisiting terephthalic acid and coumarin as probes for photoluminescent determination of hydroxyl radical formation rate in heterogeneous photocatalysis, Appl. Catal. A Gen. 598 (2020) 117566, https://doi.org/10.1016/j.apcata.2020.117566.
[19] H. Warsahartana, A. Basir, A. Keyworth, R. Davis, M. Falkowska, E. Asuquo, S. Edmondson, A. Garforth, Catalytic steam hydrolysis of polyethylene

terephthalate to terephthalic acid followed by repolymerisation, Chem. Eng. Trans. 100 (2023) 445–450, https://doi.org/10.3303/CET23100075.
[20] W. Yang, R. Liu, C. Li, Y. Song, C. Hu, Hydrolysis of waste polyethylene terephthalate catalyzed by easily recyclable terephthalic acid, Waste Manag 135 (2021) 267–274, https://doi.org/10.1016/j.wasman.2021.09.009.
[21] C. D'Agostino, J. Mitchell, M.D. Mantle, L.F. Gladden, Interpretation of NMR relaxation as a tool for characterising the adsorption strength of liquids inside porous materials, Chem. Eur. J. 20 (2014) 13009–13015, https://doi.org/10.1002/chem.201403139.
[22] R.A. Spurr, H. Myers, Quantitative analysis of anatase-rutile mixtures with an x-ray diffractometer, Anal. Chem. 29 (1957) 760–762, https://doi.org/10.1021/ac60125a006.
[23] T.F. Berto, K.E. Sanwald, W. Eisenreich, O.Y. Gutiérrez, J.A. Lercher, Photoreforming of ethylene glycol over Rh/TiO_2 and Rh/GaN:ZnO, J. Catal. 338 (2016) 68–81, https://doi.org/10.1016/j.jcat.2016.02.021.
[24] K.E. Sanwald, T.F. Berto, W. Eisenreich, O.Y. Gutiérrez, J.A. Lercher, Catalytic routes and oxidation mechanisms in photoreforming of polyols, J. Catal. 344 (2016) 806–816, https://doi.org/10.1016/j.jcat.2016.08.009.
[25] D.F. Ollis, Kinetics of photocatalyzed reactions: five lessons learned, Front. Chem. 6 (2018), https://doi.org/10.3389/fchem.2018.00378.
[26] C. Wu, A. De Visscher, I.D. Gates, Reactions of hydroxyl radicals with benzoic acid and benzoate, RSC Adv. 7 (2017) 35776–35785, https://doi.org/10.1039/C7RA05488B.
[27] M. Buchholz, M. Xu, H. Noei, P. Weidler, A. Nefedov, K. Fink, Y. Wang, C. Wöll, Interaction of carboxylic acids with rutile TiO_2(110): IR-investigations of terephthalic and benzoic acid adsorbed on a single crystal substrate, Surf. Sci. 643 (2016) 117–123, https://doi.org/10.1016/j.susc.2015.08.006.
[28] H. Sheng, H. Ji, W. Ma, C. Chen, J. Zhao, Direct four-electron reduction of O_2 to H_2O on TiO_2 surfaces by pendant proton relay, Angew. Chem. Int. Ed. 52 (2013) 9686–9690, https://doi.org/10.1002/anie.201304481.
[29] R.W. Matthews, The radiation chemistry of the terephthalate dosimeter, Radiat. Res. 83 (1980) 27–41, https://doi.org/10.2307/3575256.
[30] L. Linxiang, Y. Abe, Y. Nagasawa, R. Kudo, N. Usui, K. Imai, T. Mashino, M. Mochizuki, N. Miyata, An HPLC assay of hydroxyl radicals by the hydroxylation reaction of terephthalic acid, Biomed. Chromatogr. 18 (2004) 470–474, https://doi.org/10.1002/bmc.339.
[31] T. Hirakawa, Y. Nosaka, Properties of O_2.- and OH. Formed in TiO_2 aqueous suspensions by photocatalytic reaction and the influence of H_2O_2 and some ions, Langmuir 18 (2002) 3247–3254, https://doi.org/10.1021/la015685a.
[32] A. Serrano-Lotina, R. Portela, P. Baeza, V. Alcolea-Rodriguez, M. Villarroel, P. Ávila, Zeta potential as a tool for functional materials development, Catal. Today 423 (2023) 113862, https://doi.org/10.1016/j.cattod.2022.08.004.
[33] A.R. Agustin, K. Tamura, Surface modification of TiO_2 nanoparticles with terephthalic acid in supercritical carbon dioxide, J. Supercrit. Fluids 174 (2021) 105245, https://doi.org/10.1016/j.supflu.2021.105245.
[34] Z. Zhang, A new method for estimating zeta potential of carboxylic acids' functionalised particles, Mol. Phys. (2023) e2260014, https://doi.org/10.1080/00268976.2023.2260014.
[35] N. Robinson, P. Bräuer, A.P.E. York, C. D'Agostino, Nuclear spin relaxation as a probe of zeolite acidity: a combined NMR and TPD investigation of pyridine in HZSM-5 (https://dio.org/), Phys. Chem. Chem. Phys. 23 (2021) 17752–17760, https://doi.org/10.1039/D1CP01515J.
[36] M. Stucchi, J.P. Korb, O. Serve, V. Livadaris, B.D. Vandegehuchte, L. Prati, Low-field ^{2}D NMR relaxometry to disclose the support-substrate interaction and surface dynamics in heterogeneous catalysis: a novel and complementary view to high field NMR relaxometry, J. Catal. 428 (2023) 115168, https://doi.org/10.1016/j.jcat.2023.115168.
[37] D. Weber, J. Mitchell, J. McGregor, L.F. Gladden, Comparing strengths of surface interactions for reactants and solvents in porous catalysts using two-dimensional NMR relaxation correlations, J. Phys. Chem. C. 113 (2009) 6610–6615, https://doi.org/10.1021/jp811246j.
[38] C. D'Agostino, M.R. Feaviour, G.L. Brett, J. Mitchell, A.P.E. York, G.J. Hutchings, M.D. Mantle, L.F. Gladden, Solvent inhibition in the liquid-phase catalytic oxidation of 1,4-butanediol: understanding the catalyst behaviour from NMR relaxation time measurements, Catal. Sci. Technol. 6 (2016) 7896–7901, https://doi.org/10.1039/c6cy01458e.
[39] C. D'Agostino, T. Kotionova, J. Mitchell, P.J. Miedziak, D.W. Knight, S.H. Taylor, G.J. Hutchings, L.F. Gladden, M.D. Mantle, Solvent effect and reactivity trend in the aerobic oxidation of 1,3-propanediols over gold supported on titania: NMR diffusion and relaxation studies, Chem. Eur. J. 19 (2013) 11725–11732, https://doi.org/10.1002/chem.201300502.
[40] C. Di Valentin, A mechanism for the hole-mediated water photooxidation on TiO_2 (1 0 1) surfaces, J. Phys. Condens. Matter 28 (2016) 074002, https://doi.org/10.1088/0953-8984/28/7/074002.
[41] Q. Yang, X. Pan, Bifunctional porous polymers bearing boronic and sulfonic acids for hydrolysis of cellulose, ACS Sustain. Chem. Eng. 4 (2016) 4824–4830, https://doi.org/10.1021/acssuschemeng.6b01102.
[42] S. Suganuma, K. Nakajima, M. Kitano, D. Yamaguchi, H. Kato, S. Hayashi, M. Hara, Hydrolysis of cellulose by amorphous carbon bearing SO_3H, COOH, and OH groups, J. Am. Chem. Soc. 130 (2008) 12787–12793, https://doi.org/10.1021/ja803983h.
[43] H. Sheng, H. Zhang, W. Song, H. Ji, W. Ma, C. Chen, J. Zhao, Activation of water in Titanium dioxide photocatalysis by formation of surface hydrogen bonds: an in situ IR spectroscopy study, Angew. Chem. Int. Ed. 54 (2015) 5905–5909, https://doi.org/10.1002/anie.201412035.
[44] M. Setvin, X. Shi, J. Hulva, T. Simschitz, G.S. Parkinson, M. Schmid, C. Di Valentin, A. Selloni, U. Diebold, Methanol on anatase TiO_2 (101): mechanistic insights into photocatalysis, ACS Catal. 7 (2017) 7081–7091, https://doi.org/10.1021/acscatal.7b02003.
[45] X. Ma, Y. Shi, J. Liu, X. Li, X. Cui, S. Tan, J. Zhao, B. Wang, Hydrogen-bond network promotes water splitting on the TiO_2 surface, J. Am. Chem. Soc. 144 (2022) 13565–13573, https://doi.org/10.1021/jacs.2c03690.